



TRI-PP-86-10  
Feb 1986

## MEASUREMENTS ON A DC VOLUME H<sup>-</sup> MULTICUSP ION SOURCE FOR TRIUMF

K.R. Kendall, M. McDonald, D.R. Mossop, P.W. Schmor, and D. Yuan  
TRIUMF, 4004 Wesbrook Mall, Vancouver, B.C., Canada, V6T 2A3

G. Dammertz and B. Piosczyk  
Kernforschungszentrum Karlsruhe GmbH, West Germany

M. Oliyo  
SIN, Villigen, Switzerland

Volume production is presently the preferred mechanism for producing bright negative beams of hydrogen or deuterium. Several laboratories are investigating multicusp plasma generators as volume H<sup>-</sup> ion sources for neutral beam injection in applications with fusion plasmas and for particle accelerators.<sup>1-4</sup> These sources are characterized by their good beam quality, i.e., low emittance, high brightness, stable output, and relatively long filament lifetimes.

Since cesium is not required in the ion source, the associated voltage breakdown problems resulting from cesium contamination of the accelerating system are avoided. These properties, along with the inherent simplicity of the volume source, make it a practical choice for high intensity accelerators. We describe here the dc H<sup>-</sup> source developed

for the TRIUMF cyclotron, and present some initial measurements on the extracted beam and plasma parameters.

### **Abstract**

We describe a dc volume H<sup>-</sup> source, employing multicusp plasma confinement, which has been constructed for use with the TRIUMF cyclotron. An extracted H<sup>-</sup> current density of 12 mA/cm<sup>2</sup> has been obtained. Beam emittance and brightness have been measured as a function of current density and beam fraction. Beam brightness values for normalized beam emittances of the order of 0.2 mm<sup>2</sup>·mrad at 81% beam fraction are typically 10 mA/(mm<sup>2</sup>·mrad)<sup>2</sup> (equivalent rms B = 223 mA/(mm<sup>2</sup>·mrad)<sup>2</sup>).

### **2. EXPERIMENTAL APPARATUS**

#### **A. Plasma chamber**

The TRIUMF ion source, shown schematically in Fig. 1, is a cylindrical full-line cusp source employing 10 lines of 3.2 kg samarium-cobalt magnets deployed axially on the outside of an all-copper water-cooled plasma chamber. The plasma chamber is divided into two regions by a strong magnetic filter ( $\int B \cdot dI = 0.2$  kG·cm) after the method of Leung et al.<sup>1</sup> Three sets of four holes allow the position of the filter to be varied axially in 19 mm steps with respect to the first electrode. A fourth position bringing the first electrode to within

(submitted to Review of Scientific Instruments)

CERN LIBRARIES, GENEVA



CM-P00067456

### **1. INTRODUCTION**

5 mm of the filter rods, is achieved by placing 1 cm spacers in the extraction electrode assembly. Four lines of magnets across the back face complete the confinement of the plasma.

The chamber body is a copper cylinder (20 cm diameter by 26 cm deep inside) with 2.5 cm walls into which the Sm-Co magnets are set. Continuous operation requires water cooling which is provided by cooling passages next to each line of magnets, allowing up to 20 kW of power dissipation. Two filaments of thoriated tungsten wire (2.4 mm diameter) are mounted on the back face extending approximately 10 cm into the plasma chamber. The vacuum weld for the water-cooled filament electrodes are protected from plasma breakdown by shielding with quartz tubes. The extraction face, which is insulated from the cusp chamber body, consists of a 20 cm diameter plasma electrode with a 6.5 mm diameter extraction aperture.

#### B. Extraction Lens

The geometry of the 25 kV extraction system is shown by the cross-section in Fig. 1. It is an axially symmetric four electrode structure similar to that employed at KfK.<sup>3</sup> The first electrode, the end plate on the plasma chamber, is usually set at approximately +3V with respect to the cusp body. The H<sup>-</sup> is extracted through the 6.5 mm hole by applying a positive 3 kV potential on the second electrode. The gap between the first and second electrode is 3 mm. Permanent magnets in the first and second electrode, arranged such that they have a *fB*dl of zero, serve to sweep the simultaneously extracted electrons from the beam while giving the heavier H<sup>-</sup> ions only a small net displacement. An additional voltage increase of ~22 kV between

the second and third electrode then brings the ion energy to 25 keV. The third electrode is held slightly positive with respect to ground in order to prevent backstreaming of low energy positive ions into the acceleration gap. The fourth electrode, held at ground, has a 4 cm long 12 mm diameter snout which serves as a conductance restriction for differential pumping purposes. The optimum dimensions of the extraction system were calculated using the computer code AXCEL.<sup>5</sup> The geometry of the extraction system can be easily modified by replacing small inserts on each electrode. The electrode material is copper and is water cooled externally.

#### C. Vacuum System

In order to reduce gas stripping in the extraction lens region and run the source at optimum gas pressure, the extraction system was designed to allow differential pumping. Two turbopumps (310 and 340 Torr 1/s H<sub>2</sub>) are located on pumping ports in the extractions system vacuum-jacket and evacuate the region between the first and fourth electrode. The last aperture in the extraction system limits the conductance into the extracted region and allows a good vacuum (1 × 10<sup>-6</sup> Torr) to be maintained along the beamline, while a flow of 15 cc/min of H<sub>2</sub> maintains a plasma chamber pressure of 7 × 10<sup>-3</sup> Torr. A 15 cm diameter diffusion pump (3700 Torr 1/s air) is mounted on the first diagnostic box immediately after the extraction system and two cryogenic pumps (1000 Torr 1/s air) are placed in boxes 2 and 4. A gate valve between diagnostic boxes 1 and 2 allows source changes without affecting the beamline vacuum.

#### D. Diagnostics

On-line tuning of the extracted beam is accomplished with the aid of the four wire scanners shown in Fig. 1. The first wire scanner is placed in a diagnostic box immediately after the extraction system.

The remaining three wire scanners are placed in diagnostic boxes downstream of a solenoid magnet. A single wire (0.5 mm diameter W) mounted on the end of a insulated arm extends into the vacuum and can be pivoted, via a bellows, through the beam from outside. The angular position of the arm is determined with the aid of a linear slide resistor attached to its outer end.

The analog signals from the wire scanners can be fed directly into a storage scope and the profiles displayed on-line. The source is tuned in this mode for minimum emittance. The current on the wire can be digitized by means of a CAMAC log linear current amplifier module (LLCAM) provided by SIN. A water cooled thermocouple wire scanner, which measures the power profile of the beam, can be placed in any of the diagnostic boxes alongside a current wire scanner and gives an independent measurement of the beam profile. This scanner served as a check that the profile given by the faster wire scanners was not distorted by low energy electrons.

An axially symmetric graduated Faraday cup, placed downstream of the fourth diagnostic box, is used to monitor the total extracted beam current and the radial profile. A water cooled Faraday cup, designed to measure total beam power as well as beam current, can be swung into the beam in the first diagnostic box. The beam power is measured calorimetrically by means of thermocouples placed in the water cooling circuit.

The beam emittance can be determined by a tomographic method with

the beam focused to form a waist at the third wire scanner. Beam profiles from the final three wire scanners are digitized and stored in a computer data file. A beam tomography program<sup>7</sup> analyzes the profile data and produces emittance plots.

An independent emittance measurement technique, developed at Los Alamos,<sup>8</sup> employing electrostatic deflecting plates located between two slits was also used. A linear feed screw allows the precise positioning of the slit detector in the beam. A portion of the beam passes through a narrow slit (0.06 mm) into a region where two parallel plates (2.8 mm gap by 38 mm long) impose a variable transverse electric field. The beam, which passes through the second slit, (0.06 mm) is detected by a Faraday cup. The plate voltage can be stepped uniformly from -500 to +500 and the cup current digitized for each voltage. The detector position is moved and a set of curves generated whose width is proportional to the angular spread of the beam at each position. A computer is then used to calculate the beam emittance as a function of beam fraction.

#### E. Power Supplies

A power supply scheme for achieving the 25 keV H<sup>-</sup> beam is shown in Fig. 2. The cusp body is held at a maximum reference potential of -25 kV by a 150 mA supply. The filaments are heated by a 300 A current regulated supply. A maximum arc power of 21 kW is provided by two 70 A - 150 V arc supplies. A feedback loop from the arc to the filament supply regulates the arc current. The floating supplies are controlled and monitored via an optical link.

### 3. INITIAL MEASUREMENTS

The wire scanner beam profiles confirm the quiescent nature of the source. The plasma oscillations as evidenced by high frequency noise on the wire profiles are less than 2% of the peak. The output of the final Faraday cup was examined on an oscilloscope and revealed only a small (~5%) high frequency component in the total extracted current.

The dependence of extracted current on source pressure displays a broad pressure optimum in agreement with observations of other sources.<sup>1-3</sup> At high pressure the extracted current eventually decreases. This decrease is not, however, due to stripping in the beam transport section. The current measured on the Faraday cup at the end of the beamline is ~97% of the total current measured with the cup in the first box, indicating that gas stripping in the beamline is negligible. Evidence that stripping is also unimportant in the extraction region was obtained by measuring the ratio of extracted beam current to power as a function of gas load. This measurement was done using the Faraday cup-calorimeter in the first box.

The extracted current scaled with the extraction aperture. Initial measurements with a 13.2 mm diameter aperture yielded an extracted current of ~4.1 mA compared to ~1.0 mA under similar conditions with the standard 6.5 mm aperture. The beam brightness, however, improved with the smaller aperture probably due to a decrease in aberrations in the extraction system.

Figure 3 shows the total extracted H<sup>-</sup> current, as measured by the graduated Faraday cup, versus arc current for an arc voltage of 145 V

with all other parameters optimized. The maximum extracted current density of 10 mA/cm<sup>2</sup> at an arc of 70 A - 145 V corresponds to a current of 3.1 mA at 10 kW of arc power. This is consistent with the value observed by the pulsed Los Alamos source.<sup>2</sup> The measurements were made with the magnetic filter rods installed in the position closest to the first electrode (5 mm). This position yielded the maximum extracted H<sup>-</sup> current while minimizing the electron contamination as evidenced by the drain currents on the second and third electrodes (typically ~15 mA).

Figure 4 shows the measured normalized beam emittance ( $\gamma\beta\varepsilon$ ) as a function of current density for the data in Fig. 3 for several beam fractions. The beam fraction is defined as the square of the measured one dimensional fraction. The emittance to a good approximation exhibits a slight linear dependence on current density. A deviation from linearity appears at the highest current densities and is due to optical distortion in the extraction system.

The emittance measurements shown in Fig. 4 were made with the slit scanning technique. Tomography measurements taken concurrently yielded typically 50% higher emittance values. The tomography method also yielded 40% higher values when calculated profiles for a beam of known emittance were used. We have, therefore, used the slit measurements in our calculation of source brightness.

The brightness data is shown in Fig. 5, as a function of extracted current density, for several beam fractions. The normalized brightness is defined as:

$$B_n = 2I_f^2/\pi^2\varepsilon_n^2 \text{ (mA/(mm•mmrad)^2)}$$
 (1)

where  $I$  is the Faraday cup current,  $f$  is the fraction of total beam within the one dimensional emittance contour and  $\varepsilon_n$  is the normalized beam emittance. The brightness is nearly constant between 3 and 10 mA/cm<sup>2</sup>. Above 10 mA/cm<sup>2</sup> lens aberrations degrade the beam and the apparent brightness falls. The linear dependence of emittance on extracted current density, if truly a property of the source and not an artifact of the extraction optics, would indicate that the source brightness will plateau between 6 and 10 mA/cm<sup>2</sup> and then gradually decline.

#### 4. CONCLUSIONS

The cusp source has proved to be operationally stable and easily tuned. The testbed measurements suggest that it should out-perform the operational Ehlers' PIG source.<sup>9</sup> We intend to move the system to a new high voltage terminal nearing completion and subject the source to the operational demands of H<sup>-</sup> production in order to examine its reliability. A second cusp body is being built to serve as a spare and will be set up on the testbed to allow further source development. We have extracted a maximum current density of ~12 mA/cm<sup>2</sup> corresponding to a total H<sup>-</sup> current of 4.2 mA. The maximum measured normalized beam brightness, 11.7 mA/(mm.mrad)<sup>2</sup> at 81% fraction and 18 mA/(mm<sup>2</sup>.mrad)<sup>2</sup> at 64% fraction, occurred at a lower extracted current density of 5.6 mA/cm<sup>2</sup>. This corresponds to a rms brightness of 223 mA/(mm<sup>2</sup>.mrad)<sup>2</sup>. The wire scanning profile technique has proved to be a fast, operationally easy, method for on-line tuning of the source. The emittance can be determined reliably over a wide range of current densities using the slit scanning technique.

#### ACKNOWLEDGEMENTS

We would like to express our gratitude for the special efforts made by P. Chigmaroff with the electronics, H. Wyngaarden on the apparatus, and M. Mouat and C. Kost in software.

## REFERENCES

### Figure Captions

1. K.N. Leung, K.W. Ehlers and R.V. Pyle, Rev. Sci. Instrum. 56, 364 (1985).
  2. R.L. York and R.R. Stevens Jr., Rev. Sci. Instrum. 55, 681 (1984).
  3. G. Dammertz, B. Płoszczyk, Proc. 4th Symp. Heat. in Toroidal Plasmas, Roma Vol. II, 1087, (1984).
  4. A.J.T. Holmes, G. Dammertz, T.S. Green, and A.R. Walker, Proc. 7th Symp. on Ion Sources and Ion Assisted Technology, Kyoto, 71 (1983).
  5. J.C. Whitton, J. Smith and J.H. Whealton, J. of Comput. Phys. 28, 408 (1978).
  6. L. Rezzonico and P. Rudolf, Data Acquisition System for Beam Probes Current, 18th European Cyclotron Progress Meeting, March (1983).
  7. O.R. Sander, G.N. Minerbo, R.A. Jameson and D.D. Chamberlin, Proc. 1979 Linear Accelerator Conference, Montauk New York, Sept. 1979, 314, BNL-51134, and U. Rohrer, SIN Private Communications.
  8. P.W. Allison, D.B. Holtkamp, and J.D. Sherman, IEEE Trans. Nucl. Sci., NS 30(4), 2204 (1983).
  9. R. Baartmen, P. Bosman, R.E. Laxdal, D. Yuan, and P.W. Schmor, G. Gendreau (ed.) Ninth Int. Conf. on cyclotrons and their appl., Caen, 1981, Les Ulis (France), les Editions de la Physique, 289, (1982).
1. Schematic diagram of the multicusp ion source, extraction system, and diagnostics geometry.
  2. Power supply connections for the source and 25 kV extraction system.
  3. Total extracted  $H^-$  beam current and density vs arc current for optimized plasma parameters at a constant arc voltage of 145 V and 25 keV extraction energy.
  4. Normalized beam emittance vs current density at several beam fractions for the data in Fig. 3.
  5. Normalized brightness vs current density at several beam fractions for the data in Fig. 2.

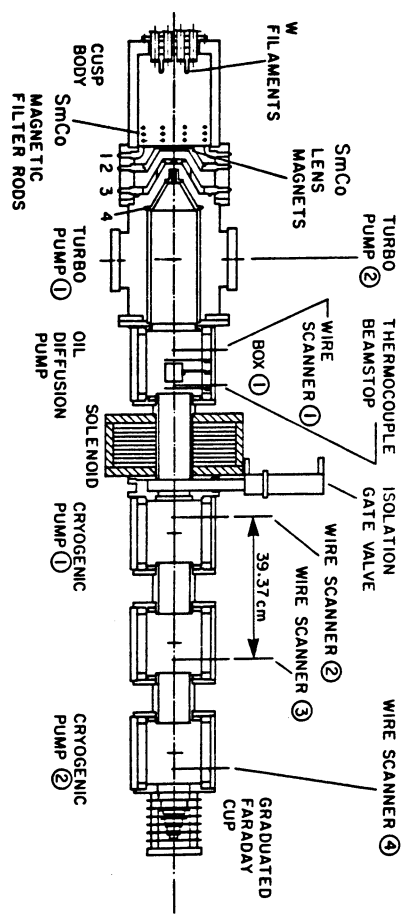


Fig. 1

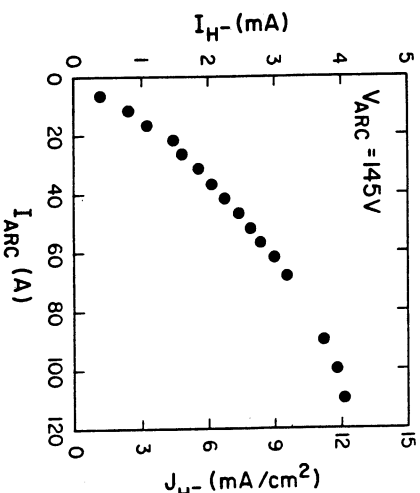


Fig. 3

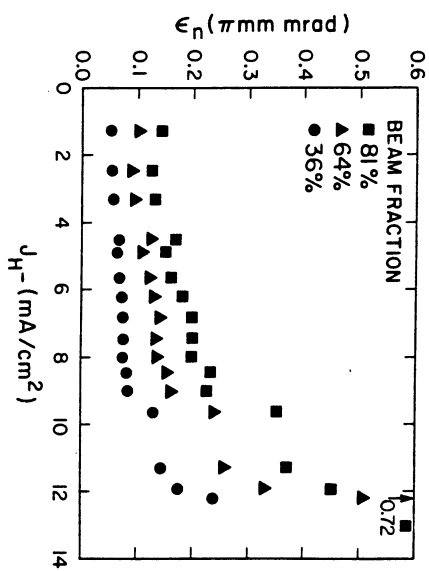


Fig. 4

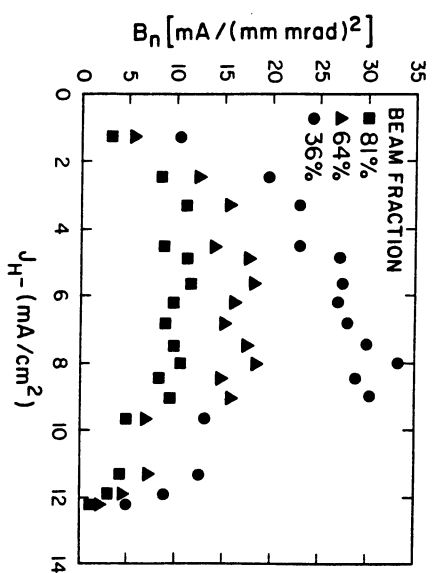


Fig. 5

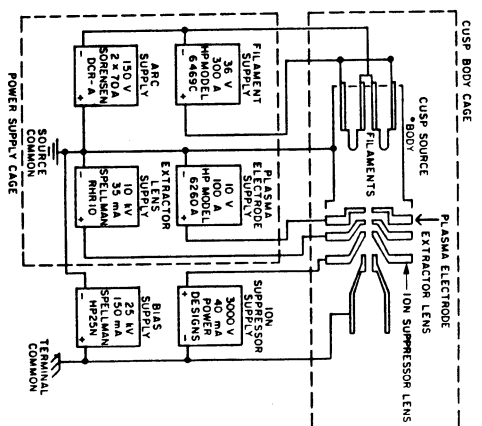


Fig. 2